Bioorganic & Medicinal Chemistry Letters 20 (2010) 1680–1684

Contents lists available at ScienceDirect

Bioorganic & Medicinal Chemistry Letters

journal homepage: www.elsevier.com/locate/bmcl

Part 2: Structure–activity relationship (SAR) investigations of fused pyrazoles as potent, selective and orally available inhibitors of p38α mitogen-activated protein kinase

Ryan P. Wurz [a,*], Liping H. Pettus [a], Bradley Henkle [b], Lisa Sherman [b], Matthew Plant [b], Kent Miner [b], Helen J. McBride [b], Lu Min Wong [b], Christiaan J. M. Saris [b], Matthew R. Lee [c], Samer Chmait [c], Christopher Mohr [c], Faye Hsieh [d], Andrew S. Tasker [a]

[a] Department of Chemistry Research & Discovery, Amgen Inc., One Amgen Center Drive, Thousand Oaks, CA 91320, USA
[b] Department of Inflammation, Amgen Inc., One Amgen Center Drive, Thousand Oaks, CA 91320, USA
[c] Department of Molecular Structure, Amgen Inc., One Amgen Center Drive, Thousand Oaks, CA 91320, USA
[d] Department of Pharmacokinetics & Drug Metabolism, Amgen Inc., One Amgen Center Drive, Thousand Oaks, CA 91320, USA

ARTICLE INFO

Article history:
Received 22 November 2009
Revised 6 January 2010
Accepted 11 January 2010
Available online 21 January 2010

Keywords:
p38
MAP kinase
TNF
Pyrazolopyridazine

ABSTRACT

A novel class of pyrazolopyridazine p38α mitogen-activated protein kinase (MAPK) inhibitors is disclosed. A structure activity relationship (SAR) investigation was conducted driven by the ability of these compounds to inhibit the p38α enzyme, the secretion of TNFα in a LPS-challenged THP1 cell line and TNFα-induced production of IL-8 in the presence of 50% human whole blood (hWB). This study resulted in the discovery of several inhibitors with IC_{50} values in the single-digit nanomolar range in hWB. Further investigation of the pharmacokinetic profiles of these lead compounds led to the identification of three potent and orally bioavailable p38α inhibitors **2h**, **2m**, and **13h**. Inhibitor **2m** was found to be highly selective for p38α/β over a panel of 402 other kinases in Ambit screening, and was highly efficacious in vivo in the inhibition of TNFα production in LPS-stimulated Lewis rats with an ED_{50} of ca. 0.08 mg/kg.

Orally active small molecules that modify the pro-inflammatory cytokine release associated with rheumatoid arthritis (RA) have generated considerable interest in the pharmaceutical industry.[1] Small molecules potentially offer a cost-effective and convenient alternative to biologics for patients and healthcare providers alike.[2] In particular, the intracellular inhibition of a number of serine/threonine and tyrosine kinases is the subject of multiple ongoing phase II clinical trials.[1]

p38α MAP kinase belongs to the serine/threonine family of kinases and is intimately involved in the signaling cascade responsible for the development of inflammation.[3] Increased activity of the p38 enzyme results in cytokine overproduction (especially IL-1β and TNFα, which is a hallmark of inflammatory disorders, such as RA, inflammatory bowel disease and psoriasis. p38 exists in four isoforms (α, β, δ, and γ) of which p38α is believed to be the predominant isoform involved in inflammation.[4] Since p38α is an integral component in the regulation of these processes, it has emerged as an attractive target for small molecule drug discovery.[5]

Recent efforts in Amgen's p38 program have been focused on a novel pyrazolopyridinone scaffold (**1**, Fig. 1).[6] The longstanding goal of our p38 program was to improve further upon kinase selectivity and this led to the exploration of structurally related[7] chemotypes to the pyrazolopyridinone class of inhibitors (**1**). Herein we report significant progress made towards this goal following the discovery of the novel pyrazolopyridazine class of p38α inhibitors, exemplified by compound **2m**.

Compounds necessary for the structure–activity relationship (SAR) study could be accessed in an expedient fashion using the two general routes illustrated in Schemes 1 and 2. Thus, ethoxy(methylene) compound (**4**) was prepared upon treatment of **3**[8] with ethyl orthoformate (69–89%, Scheme 1).[9] Condensation of **4** with the desired aryl hydrazine furnished pyrazole **5** in modest

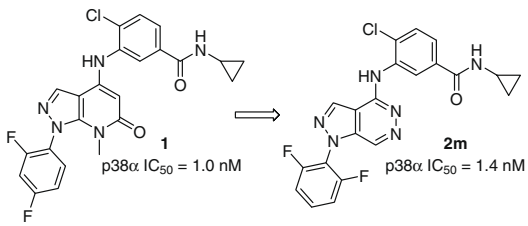

Figure 1. Fused pyrazole-derived p38 inhibitors.

* Corresponding author. Tel.: +1 805 313 5400; fax: +1 805 480 1337.
E-mail address: rwurz@amgen.com (R.P. Wurz).

0960-894X/$ - see front matter © 2010 Elsevier Ltd. All rights reserved.
doi:10.1016/j.bmcl.2010.01.059

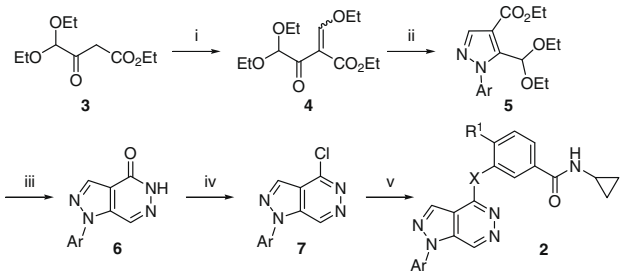

Scheme 1. General synthetic route used to access aniline NH- and O-linked pyrazolopyridazine benzamides **2**. Reagents and conditions: (i) Ac_2O, $(EtO)_3CH$, 130 °C; (ii) $ArNHNH_2$, EtOH, 0 °C to rt; (iii) NH_2NH_2, AcOH, 90 °C; (iv) $POCl_3$, 100 °C; (v) X = NH: R–NH_2, $Pd_2(dba)_3$, Dave-Phos, LiHMDS, THF, 60 °C; X = O: R–OH, $Pd_2(dba)_3$, *t*-Bu_2X-Phos, K_3PO_4, PhMe/THF 5:1, μwave, 120 °C.

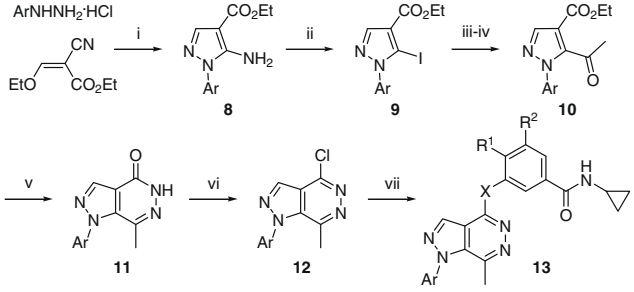

Scheme 2. General synthetic route used to access the aniline NH- and O-linked pyrazolo-7-methylpyridazine benzamides **13**. Reagents and conditions: (i) Et_3N, EtOH, reflux; (ii) isopentylONO, I_2, $CHCl_3$, reflux; (iii) $PdCl_2[P(o\text{-tol})_3]_2$, 1-ethoxyvinylSn$Bu_3$, 120 °C; (iv) HCl, rt; (v) NH_2NH_2, EtOH, reflux; (vi) $POCl_3$, PhCl, 90 °C; (vii) X = NH: R–NH_2, $Pd_2(dba)_3$, Dave-Phos, LiHMDS, THF, 60 °C; X = O: R–OH, $Pd_2(dba)_3$, *t*-Bu_2X-Phos, K_3PO_4, PhMe/THF 5:1, μwave, 120 °C.

yields (40–76%).[8] Treatment with hydrazine in acetic acid which resulted in deprotection of the acetal and cyclization to the desired pyrazolopyridazinone **6** (36–72%).[10] Chlorination of **6** with phosphorus oxychloride afforded the common chloride coupling partner (**7**, 8–42%)[9] necessary for either the Buchwald–Hartwig amination (15–87%)[11] or etherification (20–60%)[12] furnishing p38 inhibitors **2**.

Building on the SAR established in the pyrazolopyridinone series[6] preliminary efforts were focused on optimization of the aryl group of the N-1 position of the pyrazolopyridazine ring, the linker atom of the benzamide top ring X, and R.[1] Our SAR investigation was driven using the inhibition of p38α, the potency in lipopolysaccharide (LPS) challenged TNFα production in a THP1 cell line and in TNFα stimulated IL-8 secretion in the presence of 50% human whole blood (hWB, Table 1) assays results.[13]

In a similar manner to the SAR observed in the pyrazolopyridinone class of p38 inhibitors,[6] the substitution pattern at the N-1 pyrazolopyridazine aryl group had only a small influence on the potency of the inhibitor in the p38α enzyme assay (Table 1, e.g., entries **2a, 2c, 2d, 2h, 2k, 2m**). This enzyme potency generally translated well into hWB potency with the most potent inhibitors favoring 2,4-Di-F-Ph (**2e–j**) or 2,6-Di-F-Ph (**2l–n**) as N-1 aryl substituents. The slight dependence on potency of the N-1 aryl substitution pattern may be related to the preference for a twisted spatial orientation of this ring with respect to the pyrazolopyridazine scaffold, favoring *ortho*-substitutions on the N-1 aryl group that allow for enhanced dispersion interactions with the hydrophobic Ala157 residue on the floor of the binding pocket (for more details see Fig. 2).

The nature of the amide portion of the inhibitor also had a small influence on the compound's potency.[6] A primary amide (**2e**) proved to be fourfold less potent than its corresponding cyclopropyl amide analogue (**2f**) in the p38α enzyme assay. The introduction of an *ortho*-chloro group (R^1 = Cl) as a replacement for an *ortho*-methyl group (R^1 = Me) on the benzamide portion of the inhibitor was generally well tolerated, resulting in equipotent compounds (e.g., **2b** vs **2c**, **2f** vs **2h**, **2i** vs **2j**, and **2l** vs **2m**). However, introduction of a fluorine atom (R^1 = F) in this position resulted in a decline in both enzyme and cellular potency (**2g**), which is consistent with previous findings.[6] Replacement of the benzamide tether atom from X = NH with X = O invariably led to a decline in hWB potency which is also consistent with the trends observed in the pyrazolopyridinone class of p38 inhibitors.[6]

Table 1
SAR of modifications to Ar, X and R^1[a]

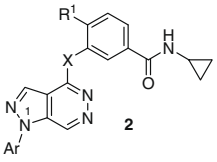

Compd	Ar	R^1	X	p38α IC_{50} (nM)	THP1 LPS/TNFα IC_{50} (nM)	hWB TNFα/IL-8 IC_{50} (nM)
2a	2-Cl-Ph	Cl	NH	1.6	4.9	26[b]
2b	3-F-Ph	Me	NH	4.6	18	76[b]
2c	3-F-Ph	Cl	NH	5.0	19	103[b]
2d	4-F-Ph	Cl	NH	8.5	25	95[b]
2e[c]	2,4-Di-F-Ph	Me	NH	12	14	30
2f	2,4-Di-F-Ph	Me	NH	3.0	2.8	7.8[b]
2g	2,4-Di-F-Ph	F	NH	43	64	176
2h	2,4-Di-F-Ph	Cl	NH	3.3	3.7	4.5[b]
2i	2,4-Di-F-Ph	Me	O	10	8.7	56
2j	2,4-Di-F-Ph	Cl	O	36	52	371[b]
2k	2,5-Di-F-Ph	Cl	NH	2.1	8.8	30[b]
2l	2,6-Di-F-Ph	Me	NH	1.7	2.1	2.6[b]
2m	2,6-Di-F-Ph	Cl	NH	1.4	1.7	6.8
2n	2,6-Di-F-Ph	Me	O	3.0	7.9	21[b]

[a] The IC_{50} data are mean values derived from at least three independent dose–response curves. Variability around the mean value was <50%.
[b] Data represents an average of two dose–response curves.
[c] Compound corresponds to a primary amide instead of a cyclopropyl amide.

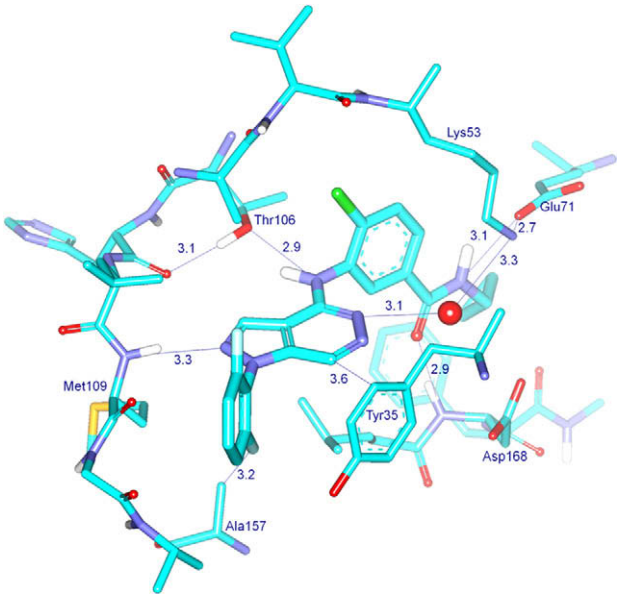

Figure 2. X-ray co-crystal structure of compound **2m** with unphosphorylated p38α.

In an attempt to improve further upon the cellular potency of compounds in this series, a methyl group was introduced at the 7-position of the pyrazolopyridazine ring. These compounds were accessed using a seven step sequence depicted in Scheme 2. Condensation of ethyl (ethoxymethylene) cyanoacetate with the desired aryl hydrazine in ethanol allowed access to 5-aminopyrazole carboxylate esters (**8**) in excellent yields (88–94%).[14] Diazotization of the amine with isopentyl nitrite and iodine in refluxing chloroform furnished the corresponding 5-iodopyrazole esters (**9**) in moderate yields (40–78%).[15] Subsequent Stille coupling of the iodide (**9**) with tributyl(1-ethoxyvinyl)tin followed by acid hydrolysis afforded the desired 5-acetyl-1*H*-pyrazole-4-carboxylic acid ethyl ester (**10**, 61–64% over 2 steps).[16] Cyclization of **10** with hydrazine furnished pyrazolopyridazinone **11** (59–82%) which was chlorinated as in Scheme 1 furnishing the common chloride coupling partners (**12**, 8–83%) for the Buchwald–Hartwig amination with the desired aniline (45–66%)[10] or etherification with the desired phenol (30–33%).[11]

Introduction of the 7-methyl group onto the pyrazolopyridazine scaffold led to a modest increase in the potency of the inhibitor resulting in several analogues with low single-digit nanomolar IC_{50} values in the hWB TNFα/IL-8 assay (Table 2, e.g., **2d** vs **13b** and **2m** vs **13h**). This improvement in potency could be attributed to the addition of favorable van der Waals interactions with the hydrophobic pocket, which may result from added stabilization of an orthogonal orientation of the pyrazolopyridazine aryl group in the aforementioned conformation that engages Ala157 with *ortho*-substituents.

The excellent in vitro potencies of p38 inhibitors **2h**, **2l**, **2m**, and **13h** prompted further profiling of their pharmacokinetic (PK) parameters in order to differentiate between these compounds for further studies (Table 3). The compounds displayed moderate to good oral bioavailability (%*F*) following oral dosing and excellent exposure (AUC) with the exception of compound **2l**. Moderate to low clearance was also observed for all four compounds. Compounds **13d** and **13h** containing a methyl group at C-7 were found to have elevated levels of human pregnane receptor X (hPXR) transactivation[17] (11% and 31% @ 2 μM, respectively) and further testing was halted. This compared unfavorably with compound **2m**, which lacked this substitution (hPXR 7% @ 2 μM).

The X-ray co-crystal structure of compound **2m** bound to unphosphorylated p38α was obtained (Fig. 2)[18] and revealed several key binding interactions. The NH of the Met109 linker engages in a hydrogen bonding interaction with N-2 of the pyrazole (3.3 Å), while the N-1 aryl group is projected into the hydrophobic pocket near the hinge region of the enzyme. The floor of this pocket contains an Ala157 residue, which according to the kinome multiple sequence alignment of Manning et al.[19] is smaller than the corresponding residue in over 98% of the catalytically active protein kinases. As discussed previously, this residue engages in a tight van der Waals contact with one of the *ortho*-fluorophenyl substituents (3.2 Å).[6] The 'gate-keeper' residue, Thr106, is internally hydrogen-bonded to the carbonyl of His107, while the oxygen lone pair participates in a hydrogen bond with the aniline NH (2.9 Å). The cyclopropyl amide forms two key interactions with Asp168 and Glu71. The amide carbonyl forms a hydrogen bond to the NH of Asp168 (2.9 Å), while the carboxylate of Glu71 forms a hydrogen bond with the NH of the cyclopropyl amide (3.1 Å). The 'DFG in' configuration (residues Asp168, Phe169, Gly170) is observed as expected.[20]

Given the superior pharmacokinetic properties to other analogs, compound **2m** was chosen for further profiling. When screened at 10 μM concentration, it was clean against a broad panel of GPCRs

Table 2
SAR of modifications to X, R^1, R^2 and Ar[a]

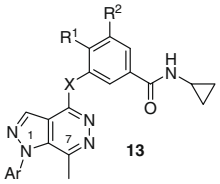

13

Compd	Ar	R^1	R^2	X	p38α IC_{50} (nM)	THP1 LPS/TNFα IC_{50} (nM)	hWB TNFα/IL-B IC_{50} (nM)[b]
13a	4-F-Ph	Me	H	NH	4.1	5.0	21
13b	4-F-Ph	Cl	H	NH	2.3	4.9	13
13c	4-F-Ph	Me	H	O	7.7	8.2	46
13d	2,4-Di-F-Ph	Me	H	NH	2.7	1.7	2.6
13e	2,4-Di-F-Ph	Me	F	NH	10	9.4	11
13f	2,4-Di-F-Ph	Cl	H	NH	1.6	2.1	3.8
13g	2,4-Di-F-Ph	Me	H	O	6.3	8.4	23
13h	2,6-Di-F-Ph	Cl	H	NH	1.7	3.2	1.8

[a] The IC_{50} data are mean values derived from at least three independent dose–response curves. Variability around the mean value was <50%.
[b] Data represents an average of two dose–response curves.

Table 3
Mean pharmacokinetic parameters for a series of compounds in male Sprague–Dawley rats[a]

Compd	iv (2.0 mg/kg in DMSO)			po (2.0 mg/kg)[b]	
	CL ((L/h)/kg)	V_{dss} (L/kg)	$t_{1/2}$ (h)	AUC(0-inf.) (ng·h/ml)	*F* (%)
2h	0.16	0.89	3.5	6550	53
2l	0.58	1.6	2.8	671	19
2m	0.22	1.1	3.6	6827	75
13h	0.47	1.4	2.2	3883	91

[a] Values are for an average of three rats.
[b] Vehicle: 1% Pluronic F68, 1% HPMC, 15% hydroxypropyl β-cyclodextrin, 83% water.

and ion channels.[21] With regard to kinase selectivity, in an Ambit screen[22] with a panel of 402 kinases, compound **2m** (@ 1 μM) hit only two kinases (POC <30%), p38α and p38β (IC_{50} = 4 nM, determined by Amgen). This exquisite kinome selectivity of **2m** is consistent with the tight van der Waals contact formed between its *ortho*-F and the Ala157 floor residue, which is smaller than 98% of the kinome.

The in vivo efficacy of compound **2m** was demonstrated in an animal disease model of LPS induced TNFα production in female Lewis rats.[23] Compound **2m** was administered at 0.01, 0.03, 0.1, and 0.3 mg/kg and resulted in an ED_{50} of ca. 0.08 mg/kg in a dose dependent manner (Fig. 3). The plasma exposure at the ED_{50} level is estimated to be between 5.5 and 5.9 ng/mL.

In conclusion, through an SAR investigation guided by previous experience with the pyrazolopyridinone class (**1**) of p38α inhibitors, a novel class of aniline NH- and O-linked pyrazolopyridazine benzamide-derived p38α inhibitors has been identified. Several compounds in this series were potent in the p38α enzyme, THP1 cell line and in TNFα challenged IL-8 secretion assays in 50% hWB. Pharmacokinetic profiling revealed that inhibitors **2h, 2m** and **13h** were orally bioavailable and displayed low clearance. The LPS induced TNFα production in female Lewis rats was used to evaluate compound **2m** in vivo, which was found to be highly efficacious with an ED_{50} of 0.08 mg/kg. In addition, compound **2m** shows excellent selectivity across a 402 member panel of kinases.

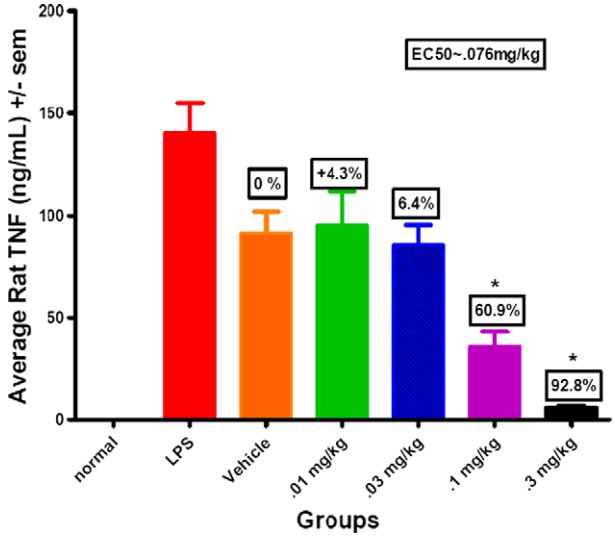

Figure 3. Effect of **2m** on LPS induced TNFα production in female Lewis rats. Vehicle or compound was dosed p.o. 60 min prior to injection with LPS IV (100 μg/rat). Blood was collected 90 min later. Serum TNFα levels were determined by ELISA (Biosource). Data points represent mean ± STE (n = 6 rats/group): (*) p < 0.01 versus vehicle control.

Acknowledgments

We acknowledge Randall Hungate and Terry Rosen for their support.

References and notes

1. Stanczyk, J.; Ospelt, C.; Gay, S. *Curr. Opin. Rheum.* **2008**, *20*, 257.
2. Chopra, P.; Kanoje, V.; Semwal, A.; Ray, A. *Expert Opin. Investig. Drugs* **2008**, *17*, 1411.
3. Schett, G.; Zwerina, J.; Firestein, G. *Ann. Rheum. Dis.* **2008**, *67*, 909.
4. O'Keefe, S. J.; Mudgett, J. S.; Cupo, S.; Parsons, J. N.; Chartrain, N. A.; Fitzgerald, C.; Chen, S.-L.; Lowitz, K.; Rasa, C.; Visco, D.; Luell, S.; Carballo-Jane, E.; Owens, K.; Zaller, D. M. *J. Biol. Chem.* **2007**, *282*, 34663.
5. For recent reviews on the design of small molecule inhibitors for p38 MAP kinase, see: (a) Pettus, L. H.; Wurz, R. P. *Curr. Top. Med. Chem.* **2008**, *8*, 1452; (b) Wagner, G.; Laufer, S. *Med. Res. Rev.* **2006**, *26*, 1; (c) Westra, J.; Limburg, P. C. *Mini-Rev. Med. Chem.* **2006**, *6*, 867; (d) Dominguez, C.; Tamayo, N.; Zhang, D. *Expert Opin. Ther. Patents* **2005**, *15*, 801; (e) Dominguez, C.; Powers, D. A.; Tamayo, N. *Curr. Opin. Drug Dis. Dev.* **2005**, *8*, 421; (f) Lee, M. R.; Dominguez, C. *Curr. Med. Chem.* **2005**, *12*, 763.
6. Wurz, R. P.; Pettus, L. H.; Xu, S.; Henkle, B.; Sherman, L.; Plant, M.; Miner, K.; McBride, H.; Wong, L. M.; Saris, C. J. M.; Lee, M. R.; Chmait, S.; Mohr, C.; McBride, H.; Hsieh, F.; Tasker, A. S. *Bioorg. Med. Chem. Lett.* **2009**, *19*, 4724.
7. For a structurally related pyrazole-derived class of p38 inhibitors see: Dyckman, A. J.; Das, J.; Leftheris, K.; Liu, C.; Moquin, R. V.; Wrobleski, S. T. US Patent 20080004278 A1, 2008.
8. Tago, K.; Arai, M.; Kogen, H. *J. Chem. Soc., Perkin Trans. 1* **2000**, 2073.
9. (a) Bisagni, E.; Bourzat, J.-D.; Marquet, J.-P.; André-Louisfert, J. *Tetrahedron* **1973**, *29*, 429; (b) Elbe, H.-L.; Gebauer, O.; Greul, J. N.; Hartmann, B.; Wachendorff-Neumann, U.; Dahmen, P.; Kuck, K.-H. WO Patent 2005042493 A1, 2005.
10. (a) Michaely, W. J.; Curtis, J. K.; Knudsen, C. G. US Patent 5300478; (b) Marquet, J.-P.; Bourzat, J.-D.; André-Louisfert, J.; Bisagni, E. *Tetrahedron* **1973**, *29*, 435.
11. Charles, M. D.; Schultz, P.; Buchwald, S. L. *Org. Lett.* **2005**, *7*, 3965.
12. Burgos, C. H.; Barder, T. E.; Huang, X.; Buchwald, S. L. *Angew. Chem., Int. Ed.* **2006**, *45*, 4321.
13. For a description of the biological assays, see: (a) Herberich, B.; Cao, G.-Q.; Chakrabarti, P. P.; Falsey, J. R.; Pettus, L.; Rzasa, R. M.; Reed, A. B.; Reichelt, A.; Sham, K.; Thaman, M.; Wurz, R. P.; Xu, S.; Zhang, D.; Hsieh, F.; Lee, M. R.; Syed, R.; Li, V.; Grosfeld, D.; Plant, M. H.; Henkle, B.; Sherman, L.; Middleton, S.; Wong, L. M.; Tasker, A. S. *J. Med. Chem.* **2008**, *51*, 6271; (b) Pettus, L. H.; Xu, S.; Cao, G.-Q.; Chakrabarti, P. P.; Rzasa, R. M.; Sham, K.; Wurz, R. P.; Zhang, D.; Middleton, S.; Henkle, B.; Plant, M. H.; Saris, C. J. M.; Sherman, L.; Wong, L. M.; Powers, D. A.; Tudor, Y.; Yu, V.; Lee, M. R.; Syed, R.; Hsieh, F.; Tasker, A. S. *J. Med. Chem.* **2008**, *51*, 6280.
14. Goldstein, D. M.; Alfredson, T.; Bertrand, J.; Browner, M. F.; Clifford, K.; Dalrymple, S. A.; Dunn, J.; Freire-Moar, J.; Harris, S.; Labadie, S. S.; La Fargue, J.; Lapierre, J. M.; Larrabee, S.; Li, F.; Papp, E.; McWeeney, D.; Ramesha, C.; Roberts, R.; Rotstein, D.; Pablo, B. S.; Sjogren, E. B.; So, O.-Y.; Talamas, F. X.; Tao, W.; Trejo, A.; Villasenor, A.; Welch, M.; Welch, T.; Weller, P.; Whiteley, P. E.; Young, K.; Zipfel, S. *J. Med. Chem.* **2006**, *49*, 1562.
15. Beck, J. R.; Gajewski, R. P.; Lynch, M. P.; Wright, F. L. *J. Heterocycl. Chem.* **1987**, *24*, 267.
16. Atkinson, R. N.; Drizin, I.; Gregg, R. J.; Gross, M. F.; Kort, M. E.; Shi, L. US Patent 20050020564 A1, 2005.
17. The compounds were tested in the PXR luciferase reporter gene assay using HepG2 cells transfected with a luciferase reporter construct driven by human CYP3A4 gene and human PXR cDNA. The incubation duration was 24 h.
18. The X-ray coordinates have been deposited in the RCSB Protein Data Bank database (RCSB ID code: RCSB054861 and PDB ID code: 3ITZ). We also thank the Advanced Light Source staff at beamline 5.0.2 for their support. The Advanced Light Source is supported by the Director, Office of Science, Office of Basic Energy Sciences, Materials Sciences Division, of the U.S. Department of Energy under Contract DE-AC03-76SF00098 at Lawrence Berkeley National Laboratory.
19. Manning, G.; Whyte, D. B.; Martinez, R.; Hunter, T.; Sudarsanam, S. *Science* **2002**, *298*, 1912.
20. For leading references and examples see: (a) Bukhtiyarova, M.; Karpusas, M.; Northrop, K.; Namboodiri, H. V. M.; Springman, E. B. *Biochemistry* **2007**, *46*, 5687; (b) Angell, R. M.; Angell, T. D.; Bamborough, P.; Bamford, M. J.; Chung, C.-w.; Cockerill, S. G.; Flack, S. S.; Jones, K. L.; Laine, D. I.; Longstaff, T.; Ludbrook, S.; Pearson, R.; Smith, K. J.; Smee, P. A.; Somers, D. O.; Walker, A. L. *Bioorg. Med. Chem. Lett.* **2008**, *18*, 4433.
21. Compound **2m** showed weak inhibition against most of the CYP 450 isoforms, with IC_{50} >27 μM for 3A4, 2D6, 2C9, 2C19, and 2D6; and moderate inhibition against 1A2 (IC_{50} = 5.4 μM). The plasma protein binding (determined by ultrafiltration methods) was measured in four species: rat, human, cynomolgus monkey, and mouse and found to be 97.1%, 97.3%, 97.6% and 96.7% protein bound, respectively.
22. Assays were performed by Ambit Biosciences (San Diego, CA: http://www.ambitbio.com/) utilizing KINOME*scan*. Activity is recorded via a competition binding assay of selected kinases that are fused to a proprietary tag. Measurements of the amount of kinase bound to an immobilized, active-

site directed ligand in the presence and absence of the test compound provide a% of DMSO control for binding of ligand. For more information on this method, see: Fabian, M. A.; Biggs III, W. H.; Treiber, D. K.; Atteridge, C. E.; Azimioara, M. D.; Benedetti, M. G.; Carter, T. A.; Ciceri, P.; Edeen, P. T.; Floyd, M.; Ford, J. M.; Galvin, M.; Gerlach, J. L.; Grotzfeld, R. M.; Herrgard, S.; Insko, D. E.; Insko, M. A.; Lai, A. G.; Lélias, J.-M.; Mehta, S. A.; Milanov, Z. V.; Velasco, A. M.; Wodicka, L. M.; Patel, H. K.; Zarrinkar P. P.; Lockhart, D. J. *Nat. Biotechnol.* **2005**, *23*, 329. Compound **2m** was screened at 1 μM and considered active if <30% of binding to immobilized probes remained compared to DMSO control.

23. Hegen, M.; Keith, J. C., Jr.; Collins, M.; Nickerson-Nutter, C. L. *Ann. Rheum. Dis.* **2008**, *67*, 1505.